Molecular Crystals and Liquid Crystals Science and Technology. Section A. Molecular Crystals and Liquid Crystals

Publication details, including instructions for authors and subscription information:
http://www.tandfonline.com/loi/gmcl19

Effect of Monomer Functionality on Performance of Holographically-Formed Polymer Dispersed Liquid Crystals

Adam K. Fontecchio [a] , Christopher C. Bowley [a] , Haiji Yuan [b] & Gregory P. Crawford [c]

[a] Brown University, Providence, Rhode Island, USA

[b] Department of Physics Division of Engineering, Palo Alto, California, USA

[c] dpiX, A Xerox New Enterprise Company, Palo Alto, California, USA

Version of record first published: 24 Sep 2006

Mol. Cryst. and Liq. Cryst., 2000, Vol. 352, pp. 399-406
Reprints available directly from the publisher
Photocopying permitted by license only

Effect of Monomer Functionality on Performance of Holographically-Formed Polymer Dispersed Liquid Crystals

ADAM K. FONTECCHIO[a], CHRISTOPHER C. BOWLEY[a], HAIJI YUAN[b] and GREGORY P. CRAWFORD[c]

[a]*Brown University, Providence, Rhode Island, USA,* [b]*Department of Physics Division of Engineering, and* [c]*dpiX, A Xerox New Enterprise Company, Palo Alto, California, USA*

Reflection gratings are formed holographically in polymer dispersed material. The effect of polymer functionality on the reflective display performance characteristics of these materials is investigated. Commercial urethane resins of functionality 2, 3, and 6 are used as base materials to create integer and half-integer effective functionalities from 2 to 6. Our results reveal an optimum reflectance at an effective functionality of 4.5.

Keywords: holography; polymer dispersed liquid crystal; functionality

INTRODUCTION

Doane and coworkers [1] pioneered the development of polymer dispersed liquid crystals (PDLCs) in the mid 1980's based on a phase separation technique. A more highly evolved form of the PDLC is the Holograhically-formed PDLC, or H-PDLC, which is formed through holographic exposure in the visible, instead of the typical UV blanket exposure. Reflection H-PDLC's show promise for application in many industries, for example fiber optics [2], diffractive optics [3], reflective displays [4], and switchable filters for remote sensing [5].

When a homogeneous mixture of pre-polymer and liquid crystal is exposed to a holographic interference pattern, rapid polymerization occurs in the bright fringes. A monomer concentration gradient is established, and monomers diffuse into the bright fringes where they are subsequently polymerized, with little polymerization occurring in the dark fringes. As the chemical potential changes, the liquid crystal becomes immiscible in the polymer and phase separation occurs. The result is a material with liquid crystal-rich droplet planes uniformly stratified through a polymer binder. Droplet density is presumably the highest where the polymerization rate is the slowest (in the dark fringes). The random orientation of droplet directors, combined with suitable choice of polymer materials, results in a refractive index mismatch between the liquid crystal-droplet rich planes and the polymer rich planes, creating a Bragg grating. Application of an electric field aligns the droplet directors, and by choosing the polymer

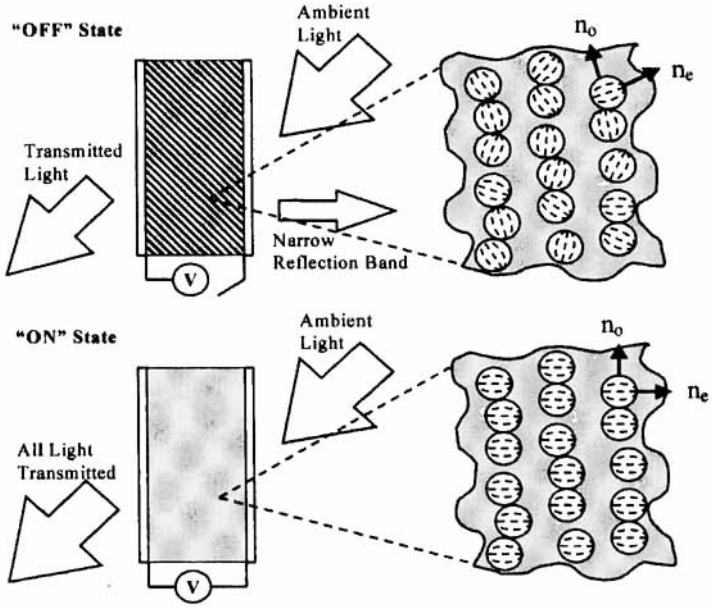

FIGURE 1 Schematic illustration showing operation of H-PDLC. The top shows the field-off, Bragg-reflecting state, and the bottom shows the field-on, transparent state.

matrix materials such that n_0 of the liquid crystal ~ n_p (the polymer index) we can "wash out" the index grating. In this case no Bragg reflection occurs, and the film is transparent to the entire visible spectrum. Both the Bragg reflecting state and the transparent state are shown in Figure 1. Gratings can be formed in both reflection [6] and transmission mode [7].

Before H-PDLCs can be effectively used in display applications, various performance characteristics need to be improved through materials optimization. This paper presents the results of an investigation centering on the effects of monomer functionality on H-PDLC performance.

For our experiment, we used commercial urethane resins of functionality 2, 3, and 6. The hexafunctional monomer yields a highly cross-linked network, while the difunctional monomer does not form a cross-linked network. The trifunctional monomer yields a network of intermediate cross-link density. We also mixed monomers of intermediate functionality using all combinations of the di-, tri-, and hexafunctional monomers.

The degree of cross-linking that exists in a network is anticipated to radically contribute to the degree of phase-separation between the liquid crystal and the polymer, producing a dramatic effect on the performance of the H-PDLC. With this in mind, we evaluated the switching properties and reflection efficiencies for integer and half-integer effective functionalities from 2 to 6. We also examined the polymer morphology through the use of scanning electron microscopy, and related the morphology to H-PDLC performance.

RESULTS

For our experiment we mixed commercial urethane resins of functionality 2, 3, and 6 to yield oligomers of intermediate functionality. Effective functionality is given by F_{eff} in the formula:

$$F_{eff} = \Sigma \varphi_i F_i$$

where φ_i is the mass fraction of oligomer functionality, F_i. Effective functionalities for all integer and half-integer combinations of 2 and 3, 2 and 6, and 3 and 6 were repeatedly heated and agitated to ensure a homogeneous pre-polymer solution. Each of these mixtures was then

combined with an initiator mixture consisting of the photoinitiator Rose Bengal, a co-initiator NPG, and a small amount of NVP. The liquid crystal BL038, obtained from EM Industries, completed the mixture.

A single-pixel electro-optic cell was created by drop-filling a small amount of each mixture between two 1"x1" ITO-coated pieces of glass. To maintain a uniform cell gap, the glass is treated with 5μm fiber spacers prior to filling. Each sample is then vacuum pressed, to achieve uniform filling. The sample is placed in a holder, and exposed to the holographic interference pattern created by two opposed beams from an Ar+ laser for ~ 20 - 30 seconds, creating a Bragg interference grating. The equation for the Bragg grating is given by:

$$\Lambda = \lambda / 2n\cos\theta$$

where λ is the laser wavelength (514 nm), n is the average index of refraction of the holographic medium, and θ is the angle between the interfering beams.

Reflection efficiency and switching voltages were measured using a SpectraScan 705 spectroradiometer. A plot of effective functionality vs. reflection efficiency is shown in Figure 2. Clearly, the 2 and 6 mixtures yield lower reflection efficiencies than the 3 and 6 mixtures at the same effective functionality. Also, reflection

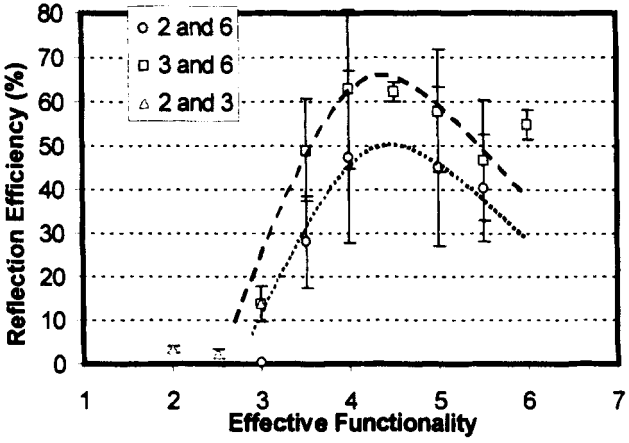

FIGURE 2 Effective functionality of monomer vs. reflection efficiency.

efficiency appears to peak for effective functionality ~ 4.5, with reflection efficiencies greater than 60%. Notice that for the 2 and 3 mixtures, with minimal or no cross-linking, the reflection efficiencies are miniscule.

Figure 3 shows the relationship between effective functionality and Δn, where

$$\Delta n = (\langle n_{\text{liquid crystal}} \rangle - n_{\text{polymer}}) / 2$$

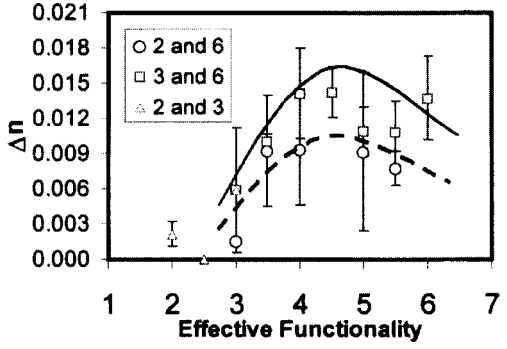

FIGURE 3 Effective functionality of monomer vs. Δn.

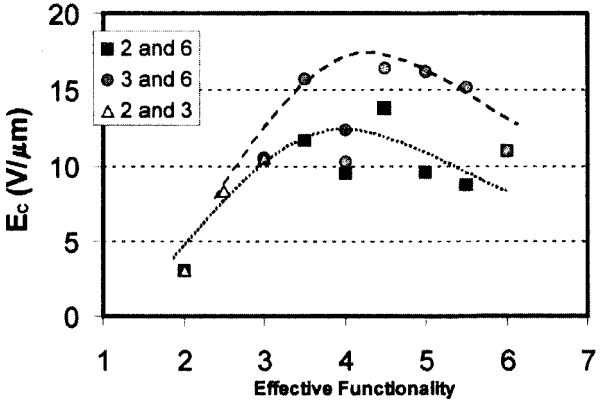

FIGURE 4 Effective functionality of monomer vs. critical electric field.

If we consider n_0 to be a constant, then we can tune our theoretical peaks by altering Δn, Λ, and the number of Bragg planes until the peak wavelength, peak reflectance, and FWHM of the experimental peaks are matched. As with the reflection efficiency, we find a peak for Δn centered on the 4.5 functionality mixture.

In Figure 4, we see the relationship between effective functionality and critical field. E_c is the field required to switch the H-PDLC to 90 % of it's zero-field reflection efficiency. As with reflection efficiency and index modulation we find a peak, this time centered at approximately $F_{eff} = 4$. The critical voltages are higher for the 3 and 6 materials than for the 2 and 6 materials. It is possible to lower the switching voltages through the use of surfactant [8]. If we do this, we find an improvement in E_c of as much as 40% in some materials.

To explore the morphology of our H-PDLCs, we examined our mixed functionality samples with a scanning electron microscope

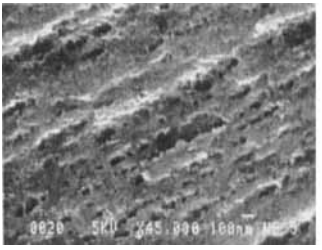

F_{eff} 4, material 2 and 6, droplet size 91± 17 nm

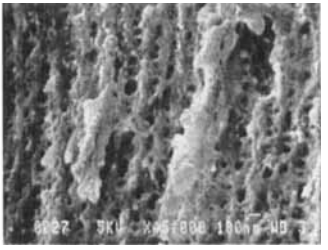

F_{eff} 4, material 3 and 6, droplet size 84 ± 23 nm

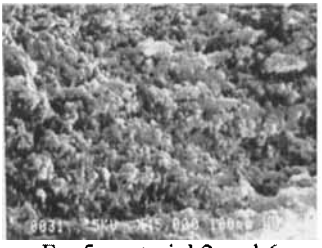

F_{eff} 5, material 2 and 6, droplet size 64 ± 14 nm

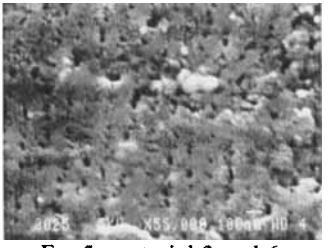

F_{eff} 5, material 3 and 6, droplet size 57 ± 14 nm

FIGURE 5 SEM micrographs of $F_{eff} = 4$ and Feff = 5 H-PDLCs.

(SEM). Figure 5 shows SEM photographs of the 4 and 5 effective functionality materials, made with both the 2 and 6 and 3 and 6 combination materials. The Bragg planes formed by alternating high and low droplet density layers are clearly visible, with droplet density in the 3 and 6 H-PDLC apparently much higher than the density in the 2 and 6 H-PDLC. This is a likely cause of the higher reflection efficiency and larger refractive index modulation that we see in the 3 and 6 materials. Droplet analysis on the SEM micrographs reveals no significant difference in droplet size between the formulations for each functionality (91 ± 17 nm for the $F_{eff} = 4$ 2 and 6 H-PDLC and 84 ± 23 nm for the 3 and 6 H-PDLC). Critical voltage for PDLCs scales as a^{-1} (a being the semi-major axis of an elliptical droplet) [9] so droplet size is not the source of the discrepancy in switching characteristics between the 2 and 6 and 3 and 6 materials.

In addition to the 514 nm exposures we exposed for the previous results, we created some exposures at a slightly different wavelength. They were cured using a 5 Watt, 532 nm laser. The H-PDLCs obtained followed the same trends as those reported above, and support the results from the 514 nm experiments.

CONCLUSION

Our study has revealed a definite connection between oligomer functionality and H-PDLC performance. The theoretical explanation for this dependence is through functionality influenced cross-linking, and our experimental data has borne this out. We combined oligomers of functionality 2, 3, and 6 to make integer and half-integer functionalities in the range from 2 through 6. Through the use of reflectance measurements, switching measurements, and scanning electron microscopy, we have shown that optimal oligomer functionality exists for the H-PDLC polymer binder. This optimum appears to have a value of $F_{eff} \sim 4$ - 4.5. While liquid crystal droplet size does not account for the switching or reflectance characteristics, SEM microscopy reveals a connection between polymer morphology and H-PDLC performance. It is a subject of future study to model the dynamics of phase separation in these systems using the Gay-Berne

potential [10] to identify the underlying physics of this observed phenomenon.

AKNOWLEDGEMENTS

We would like to gratefully acknowledge the support of dpiX, A Xerox New Enterprise Company, and DARPA under the co-operative agreement F33615-96-2-1940, and the Rhode Island Space Grant.

References

[1] G. P. Crawford and S. Zumer, in *Liquid Crystals in Complex Geometries,* Taylor and Francis, London (1996).
[2] L. Domash, *et. al., SPIE Proceedings Vol. 3010: Diffractive and holographic Device Technologies and Applications IV,* (1997).
[3] L. Domash, P. Haugsjaa, and B. E. Little, *SPIE Proceedings Vol. 3234: Design and Manufacturing of WDM Devices,* (1998).
[4] G. P. Crawford, T. G. Fiske, and L. S. Silverstein, *Digest of Technical Papers of 1996 Society for Information Display International Symposium,* p99 (1996).
[5] G. P. Crawford and J. Whitehead, Private Communication, 1999.
[6] R. L. Sutherland, L. V. Natarajan, V. P. Tondiglia, and T. Bunning, *J. Chem Mater.,* **5,** 1533 1538 (1993).
[7] K. Tanaka, K. Kato, S. Tsuru, and S. Sakai, *J. Soc. Inf. Disp.* **2**, 37 -40 (1994).
[8] H. Yuan, *et. al., Proc. Asia Display'98,* **98,** 1136 – 1139 (1998).
[9] B.-G. Wu, J. H. Erdmann, and J. W. Doane, *J. Liq. Cryst.,* **5** 1453 -1465 (1989).
[10] J. Billeter and R. Pelcovits, *Computers in Physics,* **12,** 440 – 448 (1998).
[11] T. J. Bunning, *et. al., J. Poly. Sci.,* **35**, 2825 – 2833 (1997).
[12] C. C. Bowley and G. P. Crawford, *SID Digest of Technical papers XXX*, **30**, (to be published 1999).
[13] C. C. Bowley, H. Yuan, and G. P. Crawford, *Proceedings of the 18th International Display Research Conference,* **18,** 851 – 854 (1998).
[14] H. Yuan, G. Hu, et al., *Proceedings of the 18th International Display Research Conference,* **18**, 1135 – 1139 (1998).